



# THE UNIVERSITY *of* EDINBURGH

## Edinburgh Research Explorer

### IMPLICATIONS OF ACI 288 ON INSITU NDT OF CONCRETE COMPRESSIVE STRENGTH

**Citation for published version:**

Forde, M, De Bold, R, Dimova, N, Kwong, J, Al-Abed, H & Pareemamun, K 2016, IMPLICATIONS OF ACI 288 ON INSITU NDT OF CONCRETE COMPRESSIVE STRENGTH. in M Forde (ed.), IMPLICATIONS OF ACI 288 ON INSITU NDT OF CONCRETE COMPRESSIVE STRENGTH., 1659, Structural Faults and Repair, Engineering Technics Press, Edinburgh.

**Link:**

[Link to publication record in Edinburgh Research Explorer](#)

**Document Version:**

Peer reviewed version

**Published In:**

IMPLICATIONS OF ACI 288 ON INSITU NDT OF CONCRETE COMPRESSIVE STRENGTH

**General rights**

Copyright for the publications made accessible via the Edinburgh Research Explorer is retained by the author(s) and / or other copyright owners and it is a condition of accessing these publications that users recognise and abide by the legal requirements associated with these rights.

**Take down policy**

The University of Edinburgh has made every reasonable effort to ensure that Edinburgh Research Explorer content complies with UK legislation. If you believe that the public display of this file breaches copyright please contact [openaccess@ed.ac.uk](mailto:openaccess@ed.ac.uk) providing details, and we will remove access to the work immediately and investigate your claim.



# IMPLICATIONS OF ACI 288 ON INSITU NDT OF CONCRETE COMPRESSIVE STRENGTH

N Dimova, J Kwong, H Al-Abed, R De Bold, & MC Forde  
 University of Edinburgh  
 School of Engineering  
 The Kings Buildings  
 Edinburgh EH9 3JL  
 UK

K Pareemamun  
 Mauritius Standards Board  
 Villa Road  
 Moka  
 Mauritius

**KEYWORDS:** Concrete, NDT, rebound hammer, ultrasonics, sonics, GPR, impact-echo, analysis, Impulse response (mobility).

**ABSTRACT**

Aging concrete in existing structures often suffers from changes in its properties as a result of continuous microstructural changes, such as reactions between the cement paste and aggregates, slow hydration and environmental influences that can cause degradation over time. These changes are not always detrimental, and the level of deterioration can be minimal if specifications are followed during the production of the concrete. However, the complex nature of the production and curing process, as well as the dependency on skilled workmanship often results in substandard quality concrete that has a tendency to degrade to undesirable levels over time. With the construction of these more complex structures, the overall aim of this paper is to evaluate the standard testing techniques used for a rapid non-invasive assessment of existing older concrete. The techniques from ACI228.1r-2003 and ACI22.2r-2013 are considered

**.Introduction**

A key issue arising in the 21st century is the need to test and evaluate concrete structures of all ages. The real challenge arises when it is either not permitted or not desirable to core the structure.

This paper considers basic non-destructive testing (NDT) techniques applicable to concrete structures, as outlined in ACI228.1r-2003 and the more sophisticated techniques listed in ACI228.2r-2013:

ACI228.1r-2003	ACI228.2r-2013
<ol style="list-style-type: none"> <li>1. Rebound number;</li> <li>2. Penetration resistance;</li> <li>3. Pullout</li> <li>4. Pull off bond strength</li> <li>5. Break-off;</li> <li>6. Ultrasonic pulse velocity (UPV)</li> <li>7. Maturity; and</li> <li>8. Cast-in-place cylinder.</li> </ol>	<ol style="list-style-type: none"> <li>1. Visual inspection</li> <li>2. Ultrasonic pulse velocity (UPV)</li> <li>3. Ultrasonic-echo</li> <li>4. Impact-echo</li> <li>5. Spectral analysis of surface waves</li> <li>6. Impulse-response</li> <li>7. Nuclear methods</li> <li>8. Magnetic and electrical methods</li> <li>9. Methods for measuring transport properties</li> <li>10. Infrared thermography,</li> <li>11. Radar</li> </ol>

Table 1: ACI228 overall techniques

For rapid on-site testing, with an aim to assess the quality and possibly the in-situ strength of older concrete the list in Table would probably be reduced to:

ACI228.1r-2003	ACI228.2r-2013
<ol style="list-style-type: none"> <li>1. Rebound number;</li> <li>2. Ultrasonic pulse velocity (UPV)</li> </ol>	<ol style="list-style-type: none"> <li>1. Visual inspection</li> <li>2. Ultrasonic pulse velocity (UPV)</li> <li>3. Ultrasonic-echo</li> <li>4. Impact-echo</li> <li>5. Spectral analysis of surface waves</li> <li>6. Impulse-response</li> <li>7. Methods for measuring transport properties</li> <li>8. Radar</li> </ol>

Table 2: ACI228 selected techniques

This paper will focus on *visual inspection, rebound hammer, ultrasonic inspection, impact echo, impulse response, sonic transmission, and ground penetrating radar (GPR)*.

### OBJECTIVES

This paper will focus on the problem of testing older concrete structures using various NDT techniques. It is often the case when performing such exercises, that no proper desk study can be done since relevant information is not always available to help the NDT evaluation. In this paper, the authors will show the difficulties encountered when using only one NDT technique.



Figure 1 Engineering Lecture Theatre

## LARGE SCALE EXPERIMENT AT THE UNIVERSITY OF EDINBURGH

A series of tests using NDT techniques were conducted at the University of Edinburgh on the concrete base of a historically protected (“listed”) building, the Engineering Lecture Theatre in the Hudson Beare Building at The King’s Buildings campus.

As can be seen in Figure 1, the building cantilevers in three directions from a relatively small concrete base.

### TEST PROCEDURES

The investigation focussed on testing of the concrete base structure of the building as this was concrete constructed in 1961. Depending on the investigation results, further testing of the superstructure could be undertaken.

To allow for comparison, numerous NDT methods were applied to the structure.

#### Mapping the structure

The vertical, south-facing, surface of the concrete base structure was mapped from ground level with a 0.5m by 0.5m grid, as shown in Figure 2. The wall begins to curve after column 10, becoming east-facing at column 22.

	1	2	3	4	5	6	7	8	9	10	11	12	13	14	15	16	17	18	19	20	21	22
A																						
B																						
C																						
D																						

*Figure 2 Surface map of structure*

#### External Visual Inspection

The concrete base structure was visually inspected and significant visible defects were photographed.



*Figure 3 Exposed reinforcement*



*Figure 4 The matrix of the structure*



*Figure 5 Discolouration of concrete surface*



*Figure 6 Minor repair on the structure*

For the reasons below, it is presumed that this construction did not have good site supervision:

- In Figure 3, where reinforcement is exposed, it can be seen that there is hardly any depth of concrete cover, only a thin film of surface mortar that has subsequently fallen off; the exposed reinforcement has also become badly corroded. According to Section 3.3 of BS 8110-1:1997 (BSI), this does not satisfy the requirement minimum cover depth to reinforcement for fire protection, or to Section A4 of BS 8500-1:2006 (British Standards Institution) for corrosion protection.
- In Figure 4, where the concrete structure curves, parts of the concrete surface have come away in layers. It is important to note that the structure was not rendered; therefore, the concrete that has detached off is from the structural concrete.
- In Figure 5, there is apparent discolouration of the concrete surface. This can be due to environmental condition, i.e., moisture penetrating the structure due to poor concreting; therefore, the concrete may suffer from carbonation.
- In Figure 6, there have been some repairs made to the concrete surface indicating poor workmanship in the initial construction.

A complete investigation of the concrete base structure was undertaken using different NDT techniques.

#### Rebound Hammer

The Schmidt rebound hammer is a surface hardness test with an empirical relationship between the strength of concrete and the rebound number reported by the hammer – subject to individual concrete mix calibration.



Equipment: Schmidt rebound hammer  
 Manufacturer: Proceq  
 Supplier: ELE International Ltd  
 Serial No: 108782

*Figure 7 Hardness tester*

The equipment used was as shown in Figure 7. At least ten hammer readings were taken from each grid location. Additional readings were taken if specific results were considered spurious.

The source of spurious results could come from incorrect use of the hammer, or if there was localised crushing of the concrete on impact.

The “three-sigma rule” (“ $3\sigma$ ”) was used to remove outliers that were outwith three standard deviations of the mean; at least five hammer results were to be within a range  $\pm 5$  in each grid. The mean hammer results were tabulated in the wall map, as can be seen in Figure 8.

	1	2	3	4	5	6	7	8	9	10	11	12	13	14	15	16	17	18	19	20	21	22
A	42	37	40	39	45	40	39	41	45	39	43	41	51	-	50	43	39	48	45	42	40	40
B	41	39	39	35	42	38	40	38	42	41	43	43	47	45	40	38	47	38	41	42	39	44
C	39	35	37	39	45	36	40	39	44	35	44	47	41	45	43	40	41	47	47	40	42	43
D	-	-	-	-	-	-	-	-	-	-	-	-	-	-	-	-	-	-	-	-	-	-

*Figure 8 Schmidt hammer results*

Each hammer is furnished with correlation curves developed by the manufacturer using standard cube specimens. However, the use of these curves is not recommended because material and testing conditions may not be similar to those used to calculate the calibration curves. In addition, there is little apparent theoretical relationship between the strength of concrete and its surface hardness.

No correlating graph was used to correlate the compressive strength. The results do indicate that the concrete is in fairly good condition; although the high variability of the results correlates well with the high variability of the visual condition of the concrete.

Therefore, this method is a good check of the uniformity of the concrete surface in a structure, useful to delineate regions in a structure of poor quality or deteriorated concrete, and also good to estimate in-place surface hardness. This work on the underside of the Lecture Theatre was not affected directly by rainwater as shown in Figure 9 (after Willets, 1958). However carbonation of the surface concrete will have affected the surface hardness.

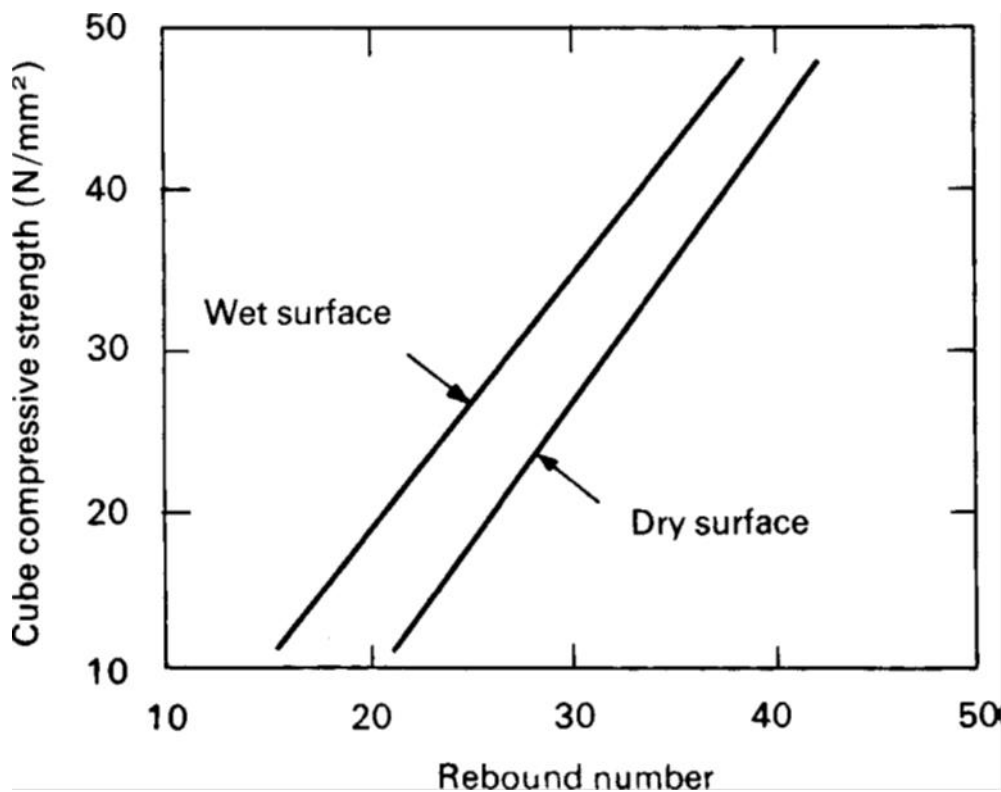


Figure 9: Influence of Surface Moisture Condition – Horizontal Hammer. (Willets, 1958)

Ultrasonic Pulse Velocity (UPV)

Ideally (BS EN 12504-4:2004), the transducer probes should be directly opposite one another, on either site of the test sample, as shown in Figure 10 (a) - the direct transmission method. Access to the opposite surface may not be possible and it will be necessary to use one of two other arrangements, i.e., the semi- direct transmission and indirect, or surface, transmission methods, as shown in Figure 10 (b) and Figure 10 (c).

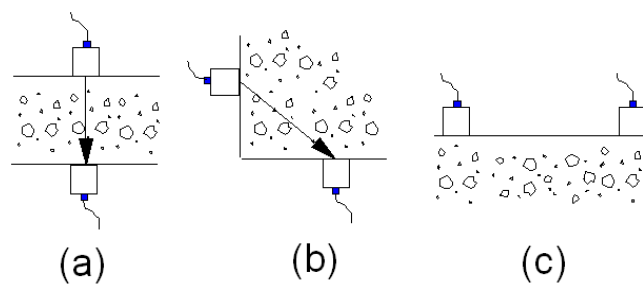


Figure 10 Ultrasonic testing techniques



Equipment: Pundit  
 Manufacturer: CNS Instruments Ltd  
 Serial No: 8622174  
 Transducer: 54MHz  
 Calibration rod 26 $\mu$ s

*Figure 11 Ultrasonic tester*

The Pundit ultrasonic tester, as seen in Figure 1, was used on the concrete base structure where the Pundit transmitter and Pundit receiver were placed on numerous different locations on its surface.

Pulse velocities obtained from surface transmission on the thick concrete were found to be between 1,905m/s to 2,325m/s. There was no discernible pattern in where different velocities occurred.

It is known that the velocity of a compression wave in concrete is between 3500 to 5000 m/s and that Rayleigh (surface) waves and shear waves are slower (by around 50%); therefore, the propagation of the waves transmitted and received by the Pundit tester on the concrete base structure were likely to be Rayleigh waves.

The Pundit tester was subsequently used on an experimental concrete slab of known parameters featuring three areas of differing reinforcement material: glass, steel and carbon. The dimensions of the slab were 1,500mm long, 1,200mm wide, and 150mm thick, as can be seen in Figure 2.

Concrete + Glass (1500mm x 400mm)
Concrete + Steel (1500mm x 400mm)
Concrete + Carbon (1500mm x 400mm)

*Figure 12 Slab reinforced with different medium*

In order to find the velocity of the surface wave, for each of the three sections of the slab, the transmitter was placed at one end and the receiver was placed 200mm from the transmitter. For each reading, the receiver was moved 200mm away from the transmitter until, for the final test, the transmitter and receiver were 1,500mm distant. This experiment was performed twice for each sections of the slab and the average velocity calculated from the plotted graph of time against distance. The velocities can be seen in Table 2.

Medium	Pulse velocity (m/s)
Concrete with Glass	2807
Concrete with Metal	3353
Concrete with Carbon	3216

*Table 2 Pulse velocity in concrete travelling in different material*



Comparing the slab experiment with the tests on the thick concrete base, it is clear that:

- (1) Conventional strategies for interpreting UPV tests assume that velocities measured are compression waves (Bungey et al, 2006).
- (2) Data reported here indicates that the velocities measured are Rayleigh surface waves.
- (3) Even converting from Rayleigh surface wave velocity to compression wave velocity is of limited value as it will be based on the near surface quality.
- (4) Thus we need to consider the amplitude of the Rayleigh wave and the resulting depth penetration of concrete assessed.

Attempting to relate UPV to concrete compressive strength is controversial. However, in the absence of calibration cores, it remains a useful NDT technique. The following section identifies certain issues and anomalies in UPV testing:

#### Transducer contact pressure:

Figure 13 illustrates the results from an experiment on smooth marble to determine the influence of transducer contact pressure:

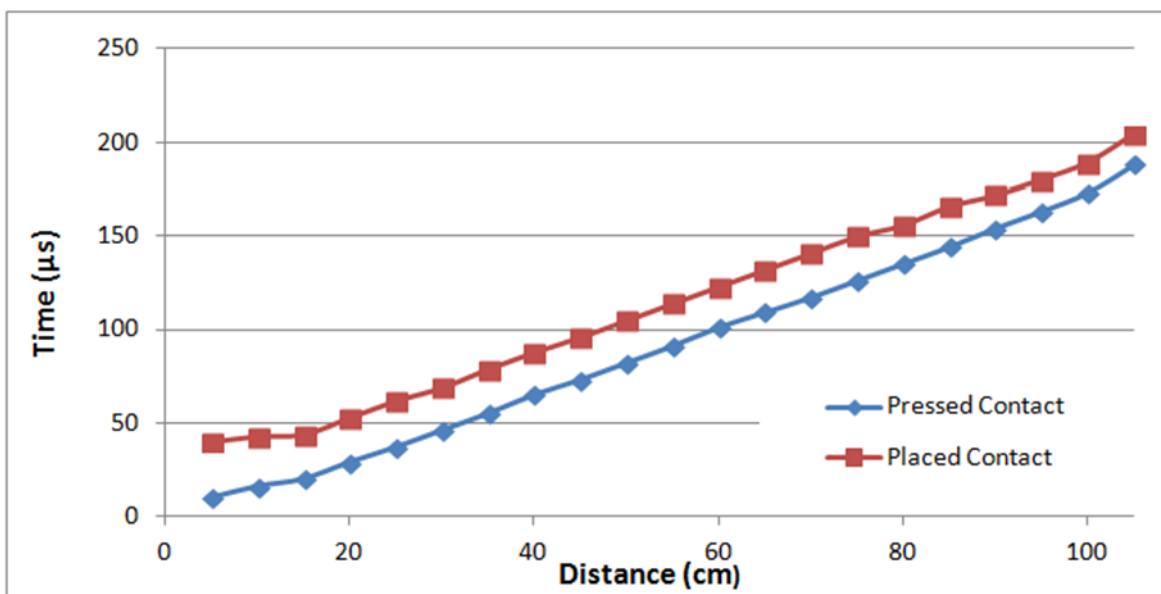


Figure 13: UPV Testing Results Marble

The clear conclusion is that firm contract pressure is required when mounting the transducer.

There is a general consideration in parts of the NDT industry that there is no credible relationship between UPV and concrete strength. However one of the objectives of this work is to examine whether more detailed analysis could aid an interpretation of UPV data. Hover (2015) has reported a 15 year study supported by the FHWA looking a correlations between “Average core strength” and UPV – see Figure 14 below.

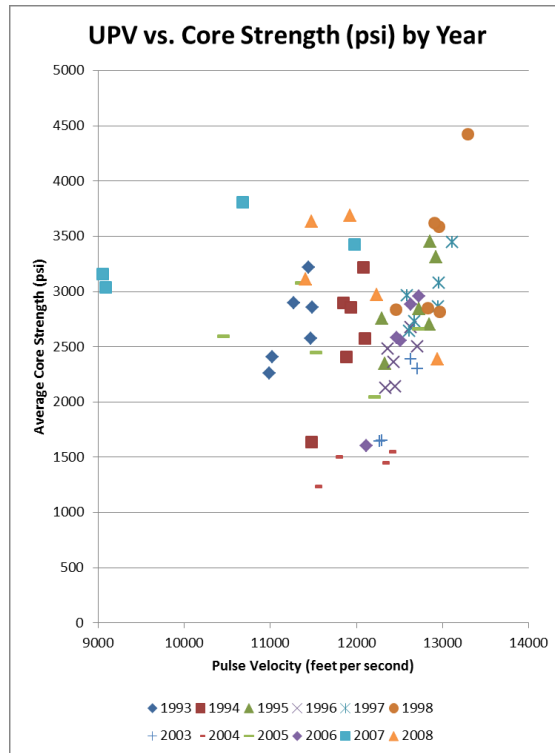


Figure 14: Average Core Strength versus Pulse Velocity (Hover, 2015)

On first inspection, this confirms the view of workers who suggest no correlation between strength and UPV. However, earlier work by Birse et al (1983) suggests that the work could be evaluated further – as proposed in the speculative Figure 15 above.

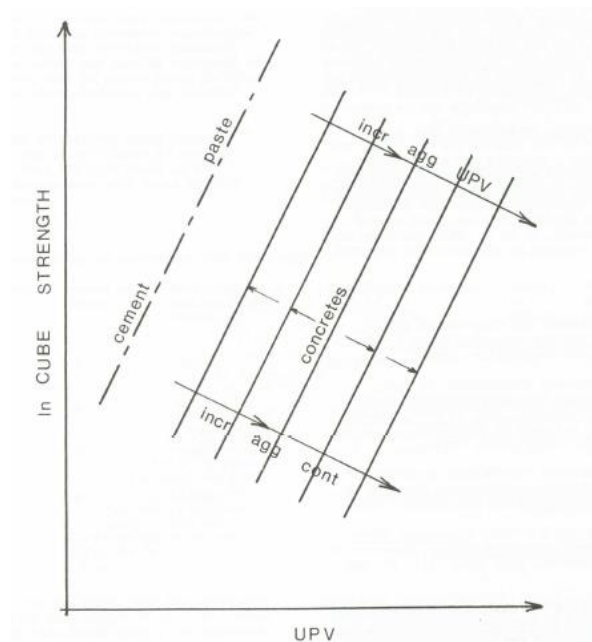


Figure 15: Idealised relationship between UPV & cube strength of concrete. (Birse, 1983)

A study was undertaken on the influence of aggregate content on UPV. The typical value for ultrasound pulse velocity of mineral admixed mortars was calculated using results for different mixtures and curing periods. The UPV values for the different types of aggregate were obtained from Rüstem Gül's paper (Appendix 1). The average UPV value for mortar (cement paste) is reported to be approximately

3500 m/s (Birse et al, 1983). That was further confirmed by Reinhardt and Christian experimental and modeling results (Reinhardt and Christian, 2005). They reported that after 80 hours, the UPV for mortar reaches a maximum value of approximately 3500 m/s.

According to Reinhardt and Christian, if concrete is considered to be a two-phase material, the two phases being concrete mortar, the UPV speed for the mix can be calculated, using the following formula:

$$\frac{1}{c_{concrete}} = \frac{V_{mortar}}{c_{mortar}} + \frac{V_{aggregate}}{c_{aggregate}}$$

Where  $c_{concrete}$  stands for P-wave speed for concrete (m/s),  $V_{mortar}$  - volume of mortar (%),  $c_{mortar}$  - P-wave speed for mortar (m/s),  $V_{aggregate}$  - volume of aggregate (%),  $c_{aggregate}$  - P-wave velocity of aggregate (m/s).

The typical aggregate content in concrete varies between 60% and 75% of its volume (Portland Cement Association, 2015). The typical compression wave velocities for different types of rocks and therefore different types of aggregate were obtained from data collected for the U.S. Department of Interior (Lucius, 2014). Therefore, the approximate average P-wave velocities for concrete mixes with a range of aggregate content can be calculated using the Formula above. The results can be seen in Table 3.

Content	100%	75%	70%	60%	50%
<b>Type of Aggregate</b>	<b>UPV (m/s)</b>				
<b>Cement Mortar (Cement Paste)</b>	3500	-	-	-	-
<b>Sandstone (Weathered)</b>	1500	2000	2100	2300	2500
<b>Sandstone (Strong)</b>	4600	4325	4270	4160	4050
<b>Shale (Weathered)</b>	2000	2375	2450	2600	2750
<b>Shale (Strong)</b>	4600	4325	4270	4160	4050
<b>Limestone (Weathered)</b>	3500	3500	3500	3500	3500
<b>Limestone (Strong)</b>	6500	5750	5600	5300	5000
<b>Igneous Rocks (Weak)</b>	4500	4250	4200	4100	4000
<b>Igneous Rocks (Strong)</b>	7000	6125	5950	5600	5250
<b>Methamorphic Rocks (Weak)</b>	3000	3125	3150	3200	3250
<b>Methamorphic Rocks (Strong)</b>	7000	6125	5950	5600	5250

Table 3: UPV for concrete mixtures with a range of aggregate contents

Birse et al (1983) presented an idealised relationship between UPV & cube strength of concrete, showing the influence of the pulse velocity in the concrete particles & the aggregate content of the concrete mix (Figure 15). From the idealised semi-logarithmic relationship, it can be seen that concretes with higher aggregate content, have higher UPV values. This is expected since, the average pulse velocity speed for

aggregates (calculated to be 4420 m/s from the values provide in Table 3) is higher than the average UPV for mortar (3500 m/s). Thus, the greater is the aggregate content, the higher the UPV for the concrete mix would be. Another trend that can be observed is that the stronger the aggregate is and thus the higher UPV it has, the higher would the UPV for the concrete mix be. This is expected, since the stronger the aggregate is, the stronger the concrete mix would be. Birse et al (1983) suggests that the relationships of pulse velocity and strength for different concretes (with different aggregates and aggregate contents) for similar curing conditions and moisture content should ideally form a family of parallel lines. It must be noted that Figure 15 is only indicative of the expected trends and does not present any quantitative relationships. This is why, it was decided to use the established strength-UPV relationship and derived pulse velocity values for different aggregate contents in order to confirm the idealised relationship and add an quantitative dimension to them.

Birse’s strength and UPV data for a range of aggregates were plotted and linear regression analysis was carried out so that a correlation between UPV and strength could be established (Figure 16). A linear relationship for UPV and compressive strength was established with an  $R^2$  value of 0.7205.

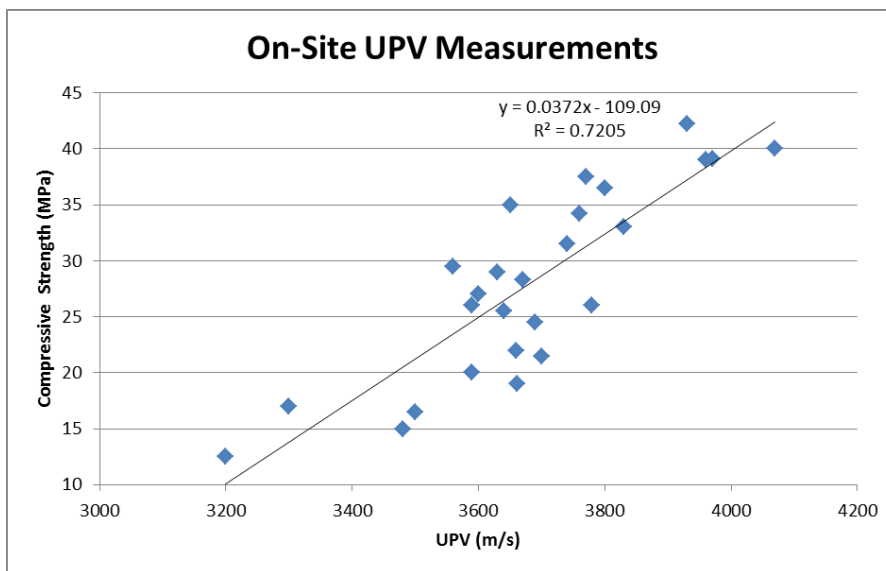


Figure 16: UPV versus Core Strength Relationship (Data from Birse et al, 1983)

Now that that the UPV values for mixtures with different aggregates and aggregate contents are known and a UPV-strength correlation was established, the relationship between aggregate content and strength can be established (Figure 17). Figure 17 does show a family of lines for four different aggregate contents, as expected. All of them have really good correlation coefficients – varying between 0.88 and 0.93. However, the lines are not parallel as expected. All four of the lines start approximately from the same origin and then branch out, indicating that for small strengths (under 15 MPa), the UPV values are not affected by aggregate content. And then, the stronger the concrete mix is (and thus aggregate in it), the more aggregate content would influence the pulse velocity of the mix.

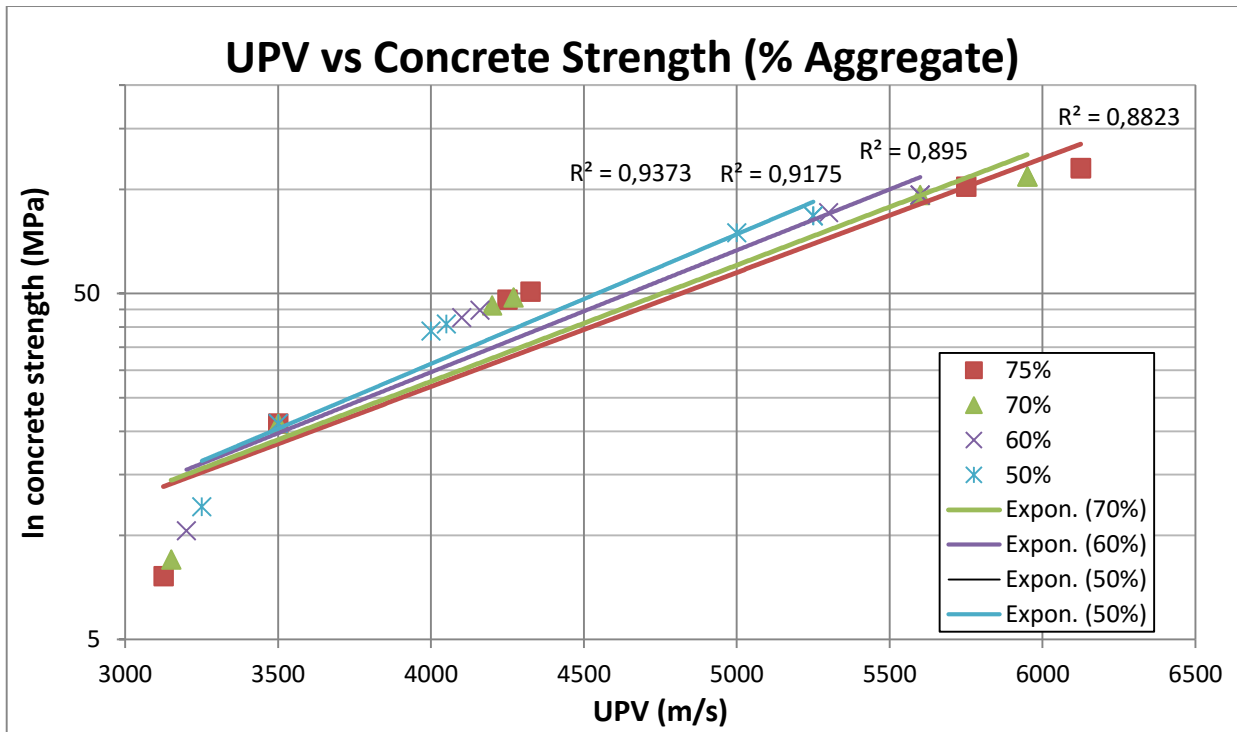


Figure 17: Influence of Aggregate Content on UPV Speed

The conclusion from this preliminary work is there is scope to undertake research into the influence of aggregate type and quantity on UPV in relation to strength.

Impact Echo

The Impact Echo testing method, as defined by ASTM C 1383 (American Society for Testing and Materials), is a non-destructive test method which relies on the effect a structure has on the propagation of stress waves. A mechanical impact to the surface of a material, generates compression, shear and surface waves. The interpretation of the measurement is analysed in the frequency domain.



Equipment: DOCTer  
 Manufacturer: Germann Instruments A/S  
 Transducer: Displacement transducer

Figure 9 Impact echo software interface

The Mark IV transducer unit was mounted on the Star support with ball impactors and connected to the computer cable. The “Viking software” interface is as can be seen in Figure 9.

The impact compression wave velocity was estimated to be 4000 m/s, and the estimated thickness of the concrete base structure was 600 mm. It is important to note that if an incorrect compression wave velocity

and concrete thickness are given, a wrong indication of the presence of a delamination or void in the concrete can also be given.

The term “flaw” is used typically by the developers of the method to describe delamination fractures and sizeable voids in the concrete being tested. The results can be seen in Figure 19.

	1	2	3	4	5	6	7	8	9	10	11	12	13	14	15	16	17	18	19	20	21	22
A	-	-	-	-	-	-	-	-	-	-	-	-	-	-	-	-	-	-	-	-	-	-
B	Flaw	Flaw	Flaw	Solid	Flaw	Flaw	Flaw	Flaw	Flaw	Flaw	Flaw	Flaw	Flaw	Flaw	Flaw	Flaw	-	-	-	-	-	-
C	Flaw	Flaw	Flaw	Flaw	Flaw	Flaw	Flaw	Flaw	Flaw	Flaw	Flaw	Flaw	Flaw	Flaw	Flaw	Flaw	-	-	-	-	-	-
D	Flaw	Solid	Flaw	Flaw	Solid	Flaw	Flaw	Flaw	Flaw	Flaw	Flaw	Solid	Flaw	Solid	Solid	Flaw	Flaw	-	-	-	-	-

Figure 19 Impact echo results on surface map

Where the impact echo method found “flaws”, there was no apparent indication of such on the surface.

The use of the impact echo test on old concrete was considered to be of little relevance to estimating concrete strength – but of considerable relevance in obtaining data on physical defects.

Impulse Response

The impulse response technique uses an impactor to send a stress wave through the tested element. The impactor is usually a modally tuned hammer with a built-in load cell in the hammerhead. Response to the input stress is normally measured using a velocity transducer (geophone). The hammer and the geophone are linked to a portable field computer for data acquisition and storage.

Both the input signal (hammer impact) and the response signal (geophone measurement) are converted into the frequency domain using a Fast Fourier Transform (FFT) algorithm. The resulting velocity spectrum is divided by the force spectrum to obtain a Frequency Response Function (FRF), referred to as the Mobility of the element under test.



Figure 20 6kg Sledge hammer

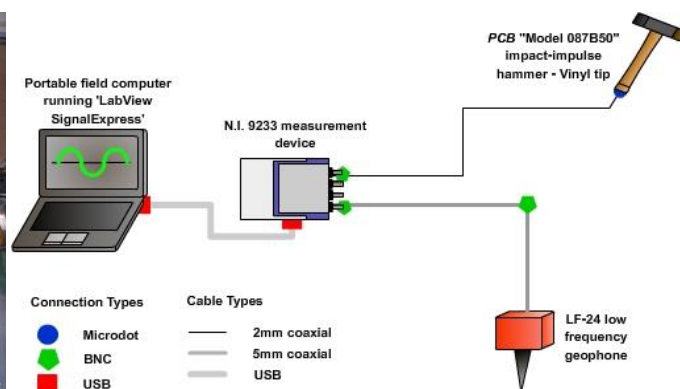


Figure 10 Experimental Setup Schematic

The impact-impulse hammer is seen in Figure 20, and equipment was setup as seen in Figure 1021.

The example graph shown in Figure 22 shows the mobility plotted against frequency of three observations over the 0Hz to 500Hz range. It can be seen that for area 7B, its mobility is less than for 7C and 7D - indicating that 7C and 7D may be subject to delamination (Davis et al, 2004). High mobility is related to delamination.

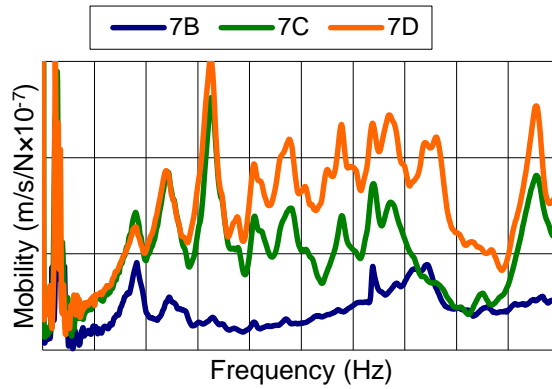


Figure 22 Mobility plot for sound and unsound system

The mobility results for all areas can be seen in Figure 23 where rows C and D are of consistently greater values.

	1	2	3	4	5	6	7	8	9	10	11	12	13	14	15	16	17	18	19	20	21	22
A	-	-	-	-	-	-	-	-	-	-	-	-	-	-	-	-	-	-	-	-	-	-
B	0.02	0.03	0.02	0.03	0.03	0.03	0.02	0.03	0.03	0.03	0.02	0.02	0.02	0.02	0.02	0.03	0.02	0.02	0.02	0.02	-	-
C	0.11	0.07	0.05	0.07	0.06	0.05	0.06	0.06	0.07	0.08	0.05	0.05	0.06	0.05	0.04	0.04	0.05	0.05	0.06	0.06	-	-
D	0.10	0.06	0.06	0.07	0.07	0.07	0.08	0.08	0.07	0.09	0.07	0.07	0.08	0.08	0.06	0.07	0.07	0.07	0.07	0.07	-	-

Figure 23 Impulse response results on surface map

The Impulse Response mode using mobility is a quick and effective means to check the integrity of the concrete – for example delaminations, voids or honeycombing. However it is not appropriate to use it in the sonic echo mode as a surface wave is created on a large surface. The technique is at its most powerful when testing concrete piles.

### Ground Penetrating Radar (GPR)

Ground Penetrating Radar (GPR) is an imaging method based on measuring reflected electromagnetic time domain waves. A transmitting dipole antenna radiates pulses into a material and a receiving antenna measures variations in the reflected signal time profile. Reflections occur as the signal moves through material interfaces between two media of differing dielectric properties.

These interface reflections give the responses from which the subsurface structural profile can be inferred. This can be seen in Figure 114, where a diagram of a layered material (left of diagram) is matched against a typical “wiggle plot” response profile (middle), and the combination of several “wiggle plots” produce radar image profile (right).

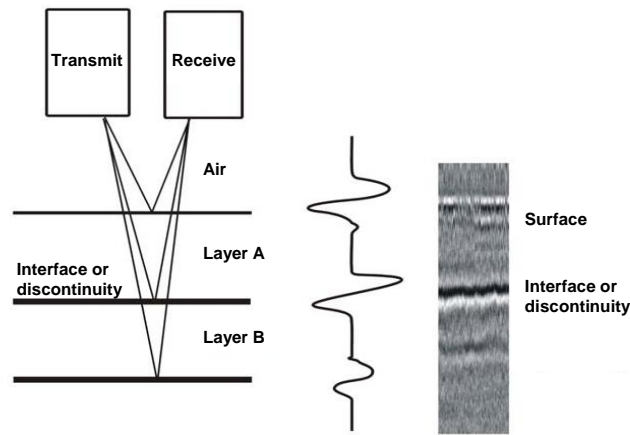


Figure 11 Generation of a GPR Profile



Equipment: SIR -3000

Manufacturer: Geophysical Survey Systems Inc (GSSI)

Software: Radan

Figure 25 GPR control unit and 1.5 GHz antenna

The equipment used is as per Figure 25. Using a high frequency radar antenna, ie, 1.5GHz, is particularly suited to locating reinforcing bars in a concrete structure due to their high reflectivity, ie, there is a great difference in electro-magnetic impedance of concrete and steel, and the high resolution relates to the high frequency used.

In favourable circumstances, this technique will indicate air voids in concrete if the latter is located in front of the reinforcing bars as can be seen in Figure 26. The void is located on the top left part of this figure with a white longitudinal wide spot, which indicates a change in phase.

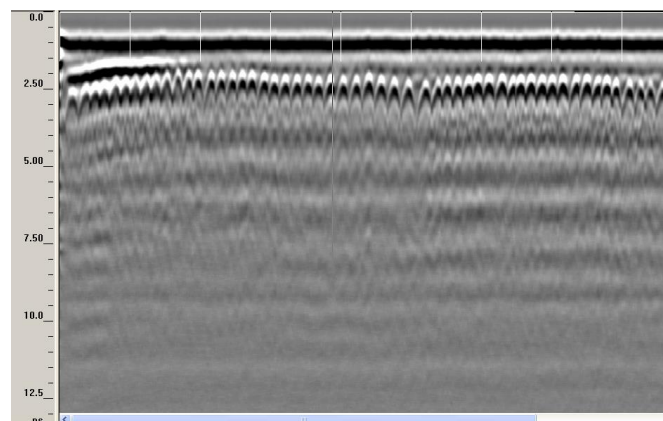


Figure 26 Surface scan featuring air void using 1.5GHz antenna

The depth to the reinforcement can be difficult to determine due to strong radar reflections from the bars obscuring the location of surface of the sample, as can be seen in Figure 27. Where a lower frequency



antenna is used on the same area, the resolution is reduced but the reinforcement is still visible, as can be seen in Figure 28

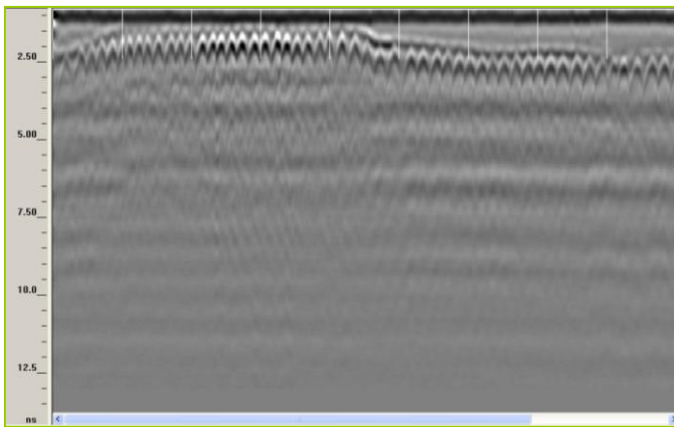


Figure 27 1.5GHz surface scan

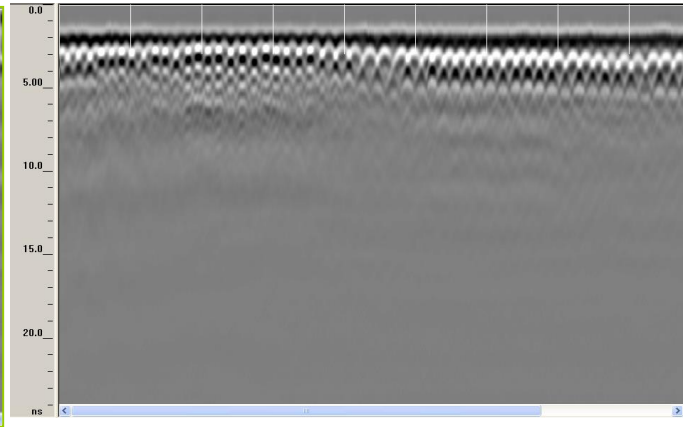


Figure 28: 900MHz surface scan

### Limitations of GPR

With very closely spaced re-bars close to the surface, GPR is not able to penetrate to any great depth. If the GPR frequency is increased to penetrate between the closely spaced re-bars, then the overall penetration depth remains low (Padaratz & Forde, 1995). Thus GPR cannot be used to estimate concrete compressive strength.

### IMPLICATIONS FOR WIDER PRACTICE WHEN TESTING OLD CONCRETE IN-SITU

When testing unknown, concrete – the investigator needs a range of techniques as demonstrated by this investigation.

However, when the investigation focuses on old concrete – where no cores may be drilled, the options are very limited. Basically there are only three readily available techniques – visual inspection, rebound hammer and ultrasonic pulse velocity. Both the latter techniques have limitations and the experimental work reported herein requires further extending.

### CONCLUSIONS

- (1) When testing unknown old concrete – the test house needs a range of NDT techniques available.
- (2) Conventional strategies for interpreting UPV tests assume that velocities measured are compression waves.
- (3) Data reported here indicates that the UPV velocities measured may well be Rayleigh surface waves.
- (4) Converting from Rayleigh surface wave velocity to compression wave velocity is of limited value as it will be based on the surface quality of the concrete. This limitation requires further research.
- (5) It is demonstrated that UPV will be related to aggregate type and content – further work is required in this area.

### ACKNOWLEDGEMENTS

All the Authors recognise the provision of facilities by The University of Edinburgh and the financial support of the IAEA. Krisna Pareemamun would like to thank the IAEA for financing his fellowship training. He would also like to thank the Government of Mauritius for nominating him for this fellowship training programme; and the Mauritius Standards Bureau for selection to attend the IAEA training course.

## REFERENCES

ACI.228.1R-03 (2003) In-Place Methods to Estimate Concrete Strength

ACI228.2R-13 (2013) Report on Nondestructive Test Methods for Evaluation of Concrete in Structures

American Society for Testing and Materials (2004) Standard Test method for Measuring the P-Wave Speed and the Thickness of Concrete Plates using the Impact-Echo Method. *ASTM C 1383-04* .

British Standards Institution. (n.d.). Concrete - Complementary British Standard to BS EN 206-1 - Part 1: Method of specifying and guidance for the specifier. *BS 8500-1:2006* .

British Standards Institution. (1997) Structural use of concrete, Part 1: Code of practice for design and construction. *BS 8110-1:1997* .

British Standards Institution. (2004). Testing concrete - Part 4: Determination of ultrasonic pulse velocity. *BS EN 12504-4:2004* .

Birse, RM, Currie, D & D Tait (1983) Ultrasonic Examination of Concrete Structures, *Proc. Int Conf Structural Faults-83*, Edinburgh, Engineering Technics Press, 1984, pp. 95-108.

Bungey, JH, Millard, SG, & Grantham, MG (2006) *Testing of Concrete in Structures*, 4<sup>th</sup> Ed, Routledge, UK

Davis, AG., Lim, MK & Petersen, CG (2004). Rapid and economical evaluation of concrete tunnel linings with impulse response and impulse radar non-destructive methods. *NDT&E International* , 38 (3), 181-186.

Hover, CK. (2015) Comparison of Non-Destructive Test Results with Core Strengths Observed in the FHWA Highway Materials Engineering Course. Cornell University. *Transportation Research Board Annual Meeting*, 2015.

Lucius, J. E. et al. (2014) An Introduction to Using Surface Geophysics to Characterize Sand and Gravel Deposits. U.S. Department of the Interior. U.S. Geological Survey. Circular 1310. Available from <[http://pubs.usgs.gov/circ/2007/1310/pdf/C1310\\_508.pdf](http://pubs.usgs.gov/circ/2007/1310/pdf/C1310_508.pdf)>

Padaratz, IJ & Forde, MC (1995) A theoretical evaluation of impulse radar wave propagation through concrete, *J. Non-destructive Testing & Evaluation*, **12**, 9-32

Reinhardt, H.W. and Christian U. G (2005) Report 31: Advanced Testing of Cement-Based Materials during Setting and Hardening – *Report of RILEM Technical Committee 185-ATC*. RILEM Publications, 2005 – Cement.

Solís-Carcaño, R. and Moreno, E.I (2008) Evaluation of concrete made with crushed limestone aggregate based on ultrasonic pulse velocity. *Construction and Building Materials Vol. 22*, pp. 1225–1231

Willetts, C.H. (1958) Investigation of the Schmidt concrete test hammer. Misc. Papers, S-627, US Army Engineer Waterways Experiment Station, Vicksburg, Miss., June 1958.